The University of Alberta
Printing Department
Edmonton, Alberta

THE UNIVERSITY OF ALBERTA

NUCLEAR QUADRUPOLE SPIN-LATTICE RELAXATION IN A SINGLE CRYSTAL OF SODIUM NITRATE

by

KENNETH REED

A THESIS

SUBMITTED TO THE FACULTY OF GRADUATE STUDIES

IN PARTIAL FULFILMENT OF THE REQUIREMENTS FOR THE

DEGREE OF MASTER OF SCIENCE

DEPARTMENT OF PHYSICS

EDMONTON, ALBERTA

JULY, 1967

UNIVERSITY OF ALBERTA

FACULTY OF GRADUATE STUDIES

The undersigned certify that they have read, and recommend to the Faculty of Graduate Studies for acceptance, a thesis entitled NUCLEAR QUADRUPOLE SPIN-LATTICE RELAXATION IN A SINGLE CRYSTAL OF SODIUM NITRATE submitted by Kenneth Reed in partial fulfilment of the requirements for the degree of Master of Science.

ACKNOWLEDGEMENTS

I wish to express my gratitude to Dr. D.G. Hughes, my research supervisor, for suggesting this project and for his patient help and encouragement throughout this work.

I also wish to acknowledge the cooperative attitude of members of the technical staff during this project.

It is a pleasure to acknowledge the National Research Council's financial support of this work.

ABSTRACT

This thesis describes an experimental study of the Na^{23} electric quadrupole spin-lattice relaxation in a single crystal of sodium nitrate.

Details are given of the construction of a modified Pound-Knight-Watkin s spectrometer and a flux-leakage balance unit. These units have been successfully operated as a crossed-coil double resonance spectrometer, allowing r-f power to be applied to the sample by means of one coil while the nuclear magnetic resonance is independently studied via a second coil which is orthogonal to the first.

Such a double resonance experiment has been performed on the Na^{23} spectrum of sodium nitrate where we have measured the enhancement of one component of the spectrum whilst saturating another. To minimise the effect of crystal imperfections we chose to saturate the centre line and observe a satellite of the resonance spectrum.

The satellite enhancement has been found to depend markedly on the spectrometer power level. By extrapolation, the value of the enhancement for infinitesimal spectrometer power has been determined.

From this, the ratio of the nuclear quadrupole spin-lattice relaxation probabilities W_2/W_1 has been found to be 2.1 ± 0.4 at room temperature and at a crystal orientation corresponding to an angle of 21.5° between the triad axis and the applied magnetic field. The significance of this result is briefly examined.

TABLE OF CONTENTS

I. INTRODUCTION

This thesis deals with some aspects of the interaction with their surroundings of a system of nuclei having a non-zero nuclear spin quantum number I. This so-called spin-lattice interaction provides the mechanism by which the nuclear spin system can return to a state of thermal equilibrium with the surroundings if the spin system is in any way disturbed. The return to equilibrium in many cases follows an exponential form allowing the definition of a characteristic relaxation time associated with the spin-lattice interaction, the so-called Longitudinal Relaxation Time T_1. In solids T_1 falls typically in the range 10^{-4} to 10^{4} seconds. For $I \geq 1$ two distinct relaxation mechanisms can occur:

i) magnetic dipole relaxation mechanism

This mechanism results from the interaction of the magnetic dipole moment of the nuclei and the fluctuating magnetic fields due to the surroundings.

ii) electric quadrupole relaxation mechanism

A nucleus with $I \geq 1$ possesses a non-zero electric quadrupole moment which interacts with the time-dependent field gradient due to

the surroundings thereby providing a relaxation mechanism.

Magnetic spin-lattice transitions are governed by the selection rule $\Delta m = \pm 1$, where m is the nuclear magnetic quantum number. In contrast, a quadrupole relaxation interaction gives rise to transitions governed by $\Delta m = \pm 2$ in addition to $\Delta m = \pm 1$. The relaxation behaviour of a nuclear spin system is thus very different in the two cases. In this thesis we shall be mainly concerned with the quadrupole relaxation interaction.

For quadrupole relaxation of a nuclear spin system with $I = 3/2$, two transition probabilities are involved. The probability of a transition $m = 3/2 \rightarrow 1/2$ is equal to the probability of a transition $m = -1/2 \rightarrow -3/2$ and is called W_1 (the transition probability $m = 1/2 \rightarrow -1/2$ being identically zero for quadrupole relaxation). Correspondingly, the transition probabilities for $m = 3/2 \rightarrow -1/2$ and for $m = 1/2 \rightarrow -3/2$ are equal and are called W_2.

The matrix elements governing the transition probabilities W_1 and W_2 involve different angular factors relative to the magnetic field direction and only in the case of a spherically symmetric electrical environment are W_1 and W_2 expected to be exactly equal. In ionic crystals where fluctuating electric field gradients arise from ionic motion

associated with lattice vibrations, a study of the relative magnitudes of W_1 and W_2 can give some insight into the nature of the lattice vibrations. In particular, anisotropy of the lattice vibrational spectrum should give rise to an orientation dependence of the ratio W_2/W_1.

For non-cubic crystals where the quadrupole interaction causes a splitting of the nuclear magnetic resonance into several components, an elegant way of measuring the ratio W_2/W_1 is by a double resonance method. In this method, one component line of the resonance spectrum is saturated while the intensities of the other components are monitored. The changes in intensity of the other components are directly related to the ratio W_2/W_1.

In this thesis we describe the construction of a double resonance spectrometer suitable for a study of the Na^{23} spin system in a single crystal of $NaNO_3$. We also present the results of preliminary measurements on $NaNO_3$ from which the ratio W_2/W_1 at one crystal orientation has been deduced.

II. THEORY

The application of a steady state magnetic field H_o to a system of nuclei with nuclear spin number I and magnetic moment μ gives rise to 2I + 1 non-degenerate Zeeman energy levels given by

$$E_m = \frac{-m\mu H_o}{I} . \qquad (1)$$

The populationsof the various energy levels in thermal equilibrium at temperature T is governed by the Boltzmann factor $\exp\left\{\frac{\Delta E}{kT}\right\}$ where ΔE is the energy difference between adjacent levels. For a nuclear spin system, the exponent $\frac{\Delta E}{kT}$ is equal to $\frac{\mu H_o}{IkT}$ and is typically $\sim 10^{-6}$ at room temperature for a field of a few thousand gauss. To excellent approximation, $\exp\left\{\frac{\Delta E}{kT}\right\}$ can therefore be written as $1 + \frac{\mu H_o}{IkT}$. It follows that if N is the total number of nuclei in the spin system under consideration the population of the mth level can be written as

$$N_m = \frac{N}{(2I + 1)}\left[1 + \frac{m\mu H_o}{IkT}\right] \qquad (2)$$

and the population difference $N_{m-1/2}$ between the mth and (m-1)th levels

is given by

$$N_{m-1/2} = N_m - N_{m-1} = \frac{N}{(2I+1)} \frac{\mu H_o}{IkT} \quad . \qquad (3)$$

Magnetic transitions governed by the selection rule $\Delta m = \pm 1$ can be induced by an applied electromagnetic field of frequency ν if the frequency is close to the resonance frequency given by $h\nu_o = \Delta E$. The probability P of such transitions takes the form (Bloembergen, Purcell and Pound, 1948)

$$P_{m \to m-1} = P_{m-1 \to m} = (1/4)\gamma_n^2 H_1^2 g(\nu)\left[I+m\right]\left[I-m+1\right] \qquad (4)$$

where $2H_1$ is the amplitude of the linearly polarised magnetic field and $g(\nu)$ is the normalised line-shape function.

Since the probability of upward and downward transitions are equal, a net absorption of energy occurs because of the slightly unequal populations of adjacent levels and the intensity of the absorption is directly proportional to the population difference.

For a spin system devoid of interaction with the outside world, the populations of the various energy levels would, in the presence of an appropriate radiation, become equal in the course of time.

In such a state, the spin system is characterised by an infinite spin temperature and the spin system is described as being completely saturated.

Of course, in reality, spin systems are never bereft of interaction with the outside world. Such an interaction, the so-called spin-lattice interaction, has a finite probability of inducing transitions. However, in this case the probability of downward transitions exceeds the probability of upward transitions (Andrew, 1955). A spin system can still be saturated by the application of radiation of sufficiently large amplitude. To illustrate this we consider the case of a spin system where $I = 1/2$. (A similar argument prevails for $I > 1/2$ if a mechanism exists for maintaining a Boltzmann distribution among the various energy levels at all times.) From equation (4) the probability of induced transitions by the electromagnetic field for the case $I = 1/2$ is

$$\underset{1/2 \rightarrow -1/2}{P} = \underset{-1/2 \rightarrow 1/2}{P} = P_o = \left(1/4\right)\gamma_n^2 H_1^2 g(\nu) . \qquad (5)$$

If the probability for upward transition is W the corresponding downward transition probability is $W\left\{1 + \frac{2\mu H_o}{kT}\right\}$ (Andrew, 1955) which we can write as $W(1 + \Delta)$. Therefore by straightforward probability arguments

$$\dot{N}_{1/2} = N_{-1/2}W(1+\Delta) + N_{-1/2}P_o - N_{1/2}W - N_{1/2}P_o$$

and $$\dot{N}_{-1/2} = N_{1/2}W + N_{1/2}P_o - N_{-1/2}W(1+\Delta) - N_{-1/2}P_o \ .$$

Since $\Delta \ll 1$ and $N_{1/2} - N_{-1/2} = N_o \ll N$, it follows that

$$\dot{N}_{1/2} = - WN_o + N_{-1/2}W\Delta - N_oP_o$$

and

$$\dot{N}_{-1/2} = WN_o - N_{-1/2}W\Delta + N_oP_o \ .$$

Hence

$$\dot{N}_o = -2WN_o - 2N_{-1/2}W\Delta - 2N_oP_o \ .$$

Now from equation (3), $N_{-1/2}\Delta$ is the equilibrium value of N_o which we denote by n_o. Therefore,

$$\dot{N}_o = 2W(n_o - N_o) - 2N_oP_o \ . \qquad (6)$$

In the absence of applied radiation the equation becomes $\dot{N}_o = 2W(n_o - N_o)$. The general solution of this type of differential equation is of the form $N_o = n_o\{1 - C\exp(-2Wt)\}$ where C is a constant determined by the initial conditions. The time constant of this exponential return to

equilibrium is $(2W)^{-1}$ which is defined as the spin lattice relaxation time T_1.

In the presence of a radiation field the steady state solution of equation (6) takes the form

$$N_o = \frac{n_o}{1 + (1/2)\gamma_n^2 H_1^2 T_1 g(\nu)} \quad . \qquad (7)$$

If H_1 is sufficiently large such that $\gamma_n^2 H_1^2 T_1 g(\nu) \gg 1$ then the spin system is said to be severely saturated.

We now consider the effect of a nuclear electric quadrupole interaction on the energy level scheme. For nuclei with an electric quadrupole moment, there is a static interaction with the field gradient due to the surroundings as well as the magnetic interaction of the nuclear magnetic dipole moment which has given the Zeeman energy levels. If the quadrupole interaction is sufficiently small compared to the Zeeman splitting then its effect can be treated by perturbation theory. A first order perturbation calculation carried out by Pound (1950) has shown that the energy levels become

$$E_m = \frac{-m\mu H_o}{I} + \frac{eQ}{4I(2I-1)}\left[3m^2 - I(I+1)\right] V_{zz} \qquad (8)$$

where eQ is the nuclear electric quadrupole moment and V_{zz} is the time average field gradient at the nuclear site with z being the direction of the external magnetic field. If the nuclei are in electrostatically equivalent environments, there are a total of 2I + 1 energy levels. Because of the dependence of the perturbation term on the value of m, the 2I successive intervals between the Zeeman energy levels are now in general no longer equal. If the environment has axial symmetry then the field gradient term is given by Pound (1950)

$$V_{zz} = (1/2)eq\left\{3\cos^2\theta - 1\right\} \qquad (9)$$

where θ is the angle between the symmetry axis of the crystal and the external magnetic field H_o. Also, eq is a scalar descriptive of the electric environment defined as

$$eq = \int \sigma \left\{3\cos^2\phi - 1\right\} r^{-3} dV \qquad (10)$$

where the integral is taken over all charges outside the nucleus, $\underline{r}$ is the vector joining the nucleus to the volume element dV, σ is the charge density and ϕ the angle between $\underline{r}$ and the symmetry axis. From equation (8) it follows that the component lines have frequencies of

$$\underset{m\rightarrow m-1}{\nu} = \nu_o + \frac{3e^2Qq}{8I(2I-1)h}(2m-1)(3\cos^2\theta - 1) \qquad (11)$$

where ν_o is the unperturbed Zeeman frequency.

For a single crystal of $NaNO_3$, the Na^{23} nuclei are in identical environments possessing axial symmetry. Since I = 3/2 for Na^{23}, the nuclear magnetic resonance consists of a spectrum of three lines. These are the so-called centre line arising from transitions $m = 1/2 \rightleftarrows -1/2$ and the so-called satellites corresponding to the transitions $m = 3/2 \rightleftarrows 1/2$ and $m = -1/2 \rightleftarrows -3/2$.

In many ionic crystals the characteristic line width of the resonance is mainly determined by nuclear magnetic dipole-dipole interactions (Van Vleck, 1948). For the case of a quadrupole split resonance, expressions for the mean square dipolar width have been given by Kambe and Ollom (1956). For the Na^{23} lines in $NaNO_3$, the theoretical Rms dipolar width is $\simeq$ 1 gauss, or in frequency units $\simeq$ 1 kc/sec, and this has been verified experimentally by Andrew etal (1962).

In the case of Na^{23} nuclei in a pure crystal of $NaNO_3$ the predominant relaxation mechanism is provided by the interaction of the nuclear quadrupole moment and the time-dependent electric field gradient,

at least near room temperature. A technique which allows the investigation of the relaxation mechanism in a single crystal of $NaNO_3$ is that due to Pound and is referred to as a 'double resonance' method. It consists of observing one component of the spectrum with a weak r-f field whilst saturating another with a large r-f field. If the relaxation processes are purely magnetic, there will be no change in the intensities of the other components of the resonance spectrum, as has been shown theoretically by Pound (1950). If on the other hand the quadrupole interaction is predominant, then there will be changes in the resonance intensities. Making some simplified assumptions this was first shown by Pound (1950).

We now consider the case of quadrupole relaxation in a slightly more general way than was done by Pound. Upward quadrupole induced spin-lattice transitions are given by (Pound, 1950, Yosida and Moriya, 1956)

$$W_{m\to m-1} = \frac{W_1(2m-1)^2(I-m+1)(I+m)}{2I(2I-1)^2} \qquad (12)$$

$$W_{m\to m-2} = \frac{W_2(I+m)(I+m-1)(I-m+1)(I-m+2)}{2I(2I-1)^2} \qquad (13)$$

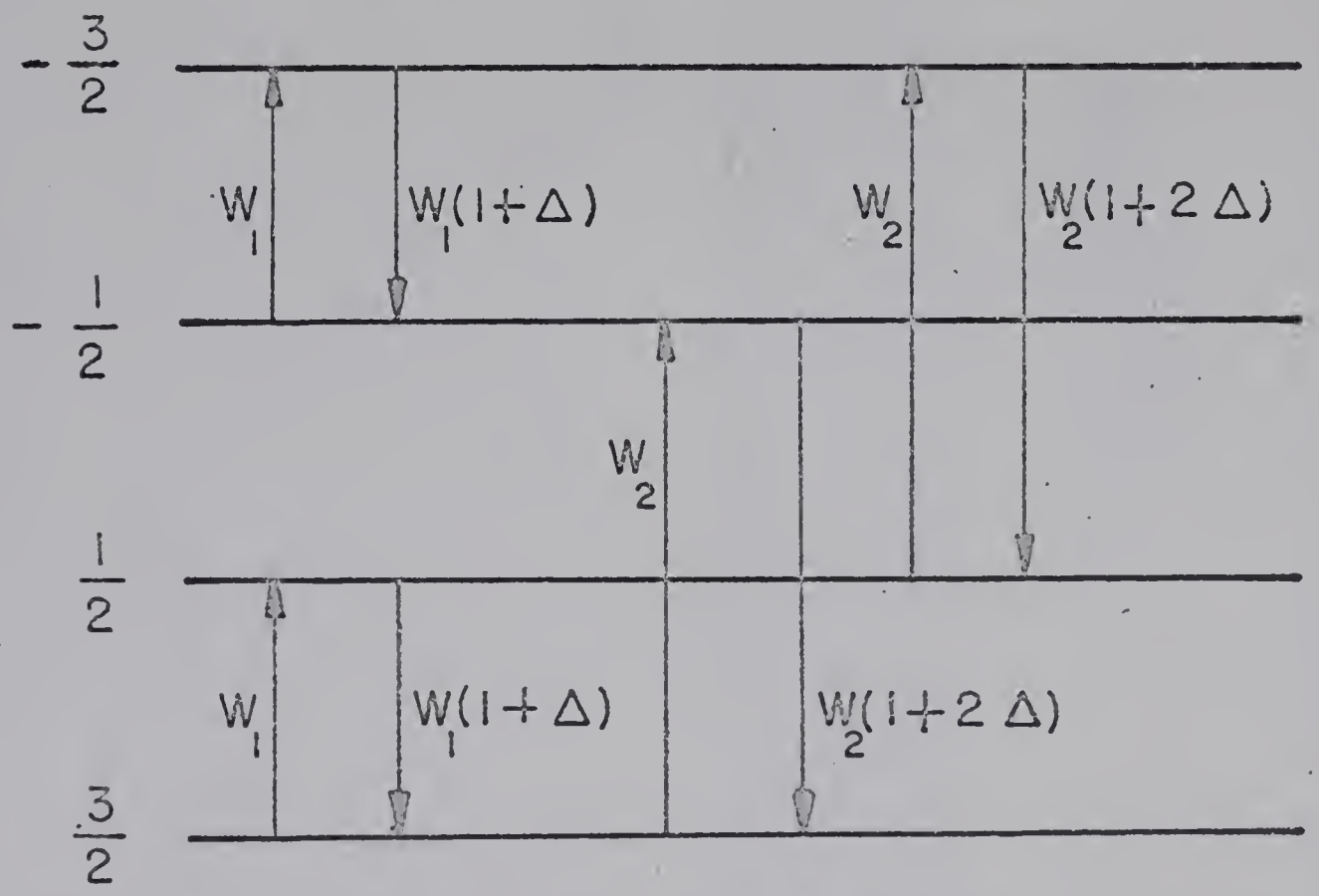

FIG. I SPIN-LATTICE TRANSITIONS FOR I= $\frac{3}{2}$

while the downward transition probabilities are given by equations (12) and (13) multiplied by the Boltzmann factors $(1 + \Delta)$ and $(1 + 2\Delta)$ respectively where $\Delta = \frac{h\nu_o}{kT}$. The transitions in the case I = 3/2 are therefore

$$\overset{W}{}_{3/2 \rightarrow 1/2} = \overset{W}{}_{-1/2 \rightarrow -3/2} = W_1, \qquad \overset{W}{}_{3/2 \rightarrow -1/2} = \overset{W}{}_{1/2 \rightarrow -3/2} = W_2,$$

$$\overset{W}{}_{1/2 \rightarrow -1/2} = 0$$ and these transitions are shown in figure I. The physical significance of W_1 and W_2 is dealt with later in this section. The probability of magnetic dipole transitions brought about by an r-f field is given by equation (4).

Consider the population dynamics for the case where all three lines in the spectrum are resolved and where power is applied to all three lines (Hughes, 1966)

$$\dot{N}_{-3/2} = -N_{-3/2}\left\{\overset{W}{}_{-3/2 \rightarrow -1/2} + \overset{P}{}_{-3/2 \rightarrow -1/2} + \overset{W}{}_{-3/2 \rightarrow 1/2}\right\} + N_{1/2}\left\{\overset{W}{}_{1/2 \rightarrow -3/2}\right\}$$

$$+ N_{-1/2}\left\{\overset{W}{}_{-1/2 \rightarrow -3/2} + \overset{P}{}_{-1/2 \rightarrow -3/2}\right\}, \qquad (14)$$

$$\dot{N}_{-1/2} = -N_{-1/2}\left\{\overset{W}{}_{-1/2 \rightarrow -3/2} + \overset{P}{}_{-1/2 \rightarrow -3/2} + \overset{W}{}_{-1/2 \rightarrow 1/2} + \overset{W}{}_{-1/2 \rightarrow 3/2}\right.$$

$$+ \underset{-1/2\to 1/2}{P}\Big\} + N_{-3/2}\Big\{\underset{-3/2\to -1/2}{W} + \underset{-3/2\to -1/2}{P}\Big\} + N_{1/2}\Big\{\underset{1/2\to -1/2}{W}$$

$$+ \underset{1/2\to -1/2}{P}\Big\} + N_{3/2}\Big\{\underset{3/2\to -1/2}{W}\Big\}, \qquad (15)$$

$$\dot{N}_{1/2} = -N_{1/2}\Big\{\underset{1/2\to -1/2}{P} + \underset{1/2\to -1/2}{W} + \underset{1/2\to -3/2}{W} + \underset{1/2\to 3/2}{W} + \underset{1/2\to 3/2}{P}\Big\}$$

$$+ N_{-1/2}\Big\{\underset{-1/2\to 1/2}{P} + \underset{-1/2\to 1/2}{W}\Big\} + N_{3/2}\Big\{\underset{3/2\to 1/2}{W} + \underset{3/2\to 1/2}{P}\Big\}$$

$$+ N_{-3/2}\Big\{\underset{-3/2\to 1/2}{W}\Big\} \qquad (16)$$

and

$$\dot{N}_{3/2} = -N_{3/2}\Big\{\underset{3/2\to 1/2}{P} + \underset{3/2\to 1/2}{W} + \underset{3/2\to -1/2}{W}\Big\} + N_{-1/2}\Big\{\underset{-1/2\to 3/2}{W}\Big\}$$

$$+ N_{1/2}\Big\{\underset{1/2\to 3/2}{P} + \underset{1/2\to 3/2}{W}\Big\}. \qquad (17)$$

For convenience we normalise with respect to W_1 as follows

$$\underset{-3/2\to -1/2}{P} = \underset{-1/2\to -3/2}{P} = 3p_{-1}W_1 ,$$

$$\underset{1/2\to -1/2}{P} = \underset{-1/2\to 1/2}{P} = 4p_0 W_1$$

and

$$\underset{1/2\to 3/2}{P} = \underset{3/2\to 1/2}{P} = 3p_1 W_1 .$$

The population differences $N_o = N_{1/2} - N_{-1/2}$, $N_1 = N_{3/2} - N_{1/2}$ and $N_{-1} = N_{-1/2} - N_{-3/2}$ are therefore, to first order, governed by the equations

$$\dot{N}_o = W_1\left\{N_{-1}(1 - x + 3p_{-1}) - N_o(2x + 8p_o) + N_1(1 - x + 3p_1) + 2n_o(2x - 1)\right\} \quad (18)$$

$$\dot{N}_1 = W_1\left\{N_{-1}(x) + N_o(4p_o) - N_1(2 + x + 6p_1) + 2n_o\right\} \quad (19)$$

$$\dot{N}_{-1} = W_1\left\{-N_{-1}(2 + x + 6p_{-1}) + N_o(4p_o) + N_1(x) + 2n_o\right\} \quad (20)$$

where n_o is the equilibrium population difference in the absence of r-f power, $x = W_2/W_1$ and the first order approximations are $n_o \simeq N_{1/2}\,\Delta$ etc. and N_o, N_1, $N_{-1} \ll N_{3/2}$, $N_{-3/2}$, $N_{1/2}$, $N_{-1/2}$.

The steady state solution of (18), (19) and (20) when $\dot{N}_o = \dot{N}_1 = \dot{N}_{-1} = 0$ gives the equilibrium population differences in the presence of r-f power as .

$$N_o = n_o\left\{2x + 2x^2 + 3p_1(3x + 2x^2) + 3p_{-1}(3x + 2x^2) + 36xp_1p_{-1}\right\}A^{-1}, \quad (21)$$

and

$$N_1 = n_o\left\{2x + 2x^2 + 4p_o(1 + 3x + 2x^2) + 3p_{-1}(2x) + 12p_op_{-1}(1 + 2x)\right\}A^{-1}, \quad (22)$$

where

$$A = \Big\{ 2x + 2x^2 + 4p_o(1 + 2x + x^2) + 3p_1(2x + x^2) + 3p_{-1}(2x + x^2)$$

$$+ 12p_o p_1(1 + x) + 12p_o p_{-1}(1 + x) + 9p_1 p_{-1}(2x) + 36p_o p_1 p_{-1} \Big\} .$$

N_{-1} is given by equation (22) with the interchange of p_1 and p_{-1}.

Consider the case when the centre line is severely saturated and the $N_{3/2} \rightarrow N_{1/2}$ satellite is observed with an r-f power p. From equation (22) the satellite population difference N_1 is given by

$$N_1 = n_o \left\{ 1 + \frac{3p(2 + x)}{2(1 + x)} \right\}^{-1} \qquad (23)$$

and, when the centre line is severely saturated ($p_o = p_{sat} \gg 1, p$),

$$N_1 = n_o(1 + 2x)(1 + x + 3p)^{-1}. \qquad (24)$$

The observed satellite enhancement E therefore is accurately given by

$$\frac{(1 + 2x)\left\{1 + 3p(2 + x)/2(1 + x)\right\}}{(1 + x)\left\{1 + 3p/(1 + x)\right\}} . \qquad (25)$$

If p is kept substantially less than unity the enhancement factor is adequately given, to first order in p, by

$$E = \frac{1 + 2x}{1 + x}\left\{1 + \frac{3px}{2(1 + x)}\right\} \quad . \tag{26}$$

By similar argument, if $N_{-1/2 \rightarrow -3/2}$ satellite is severely saturated then the enhancement factor for the centre line, to first order in p, is given by

$$\frac{3 + 2x}{2 + x}\left\{1 + \frac{2p(1 + x)}{2 + x}\right\} \tag{27}$$

whilst the $N_{3/2 \rightarrow 1/2}$ satellite is depressed by a factor

$$\frac{2}{2 + x}\left\{1 + \frac{3px^2}{2(1 + x)(2 + x)}\right\} \quad . \tag{28}$$

In his original treatment of enhancement ratios, Pound (1950) assumed that $W_2 = W_1$. He also did not include the effect of a finite observing power. To this approximation ($x = 1$, $p = 0$), the theoretical enhancement ratio of a satellite when the centre line is severely saturated is 1.5. While the signal-to-noise ratio of Pound's resonances is no better than about 5 to 1, nevertheless the observed enhancement does seem significantly greater than 1.5, probably close to 1.75 (Abragam, 1961). However, Pound's data does not necessarily imply that the ratio W_2/W_1 is significantly greater than unity. Inspection of

equation (26) shows that if the observing power p had a value of 0.1 to 0.2 (a not unreasonable value) then W_2/W_1 could well be close to unity for Pound's particular crystal orientation.

It is clear that to obtain an accurate value of W_2/W_1 it is necessary to measure the enhancement ratio E as a function of observing power to determine the enhancement ratio in the limit of vanishing p by extrapolation.

We shall now consider the physical significance of W_1 and W_2. The matrix elements of the quadrupole Hamiltonian are given by (Cohen and Reif, 1957)

$$\begin{aligned}
\langle m|H_Q|m\rangle &= A\left\{3m^2 - I(I+1)\right\}V_o \\
\langle m \pm 1|H_Q|m\rangle &= A\left\{2m \pm 1\right\}\left[\left\{I \mp m\right\}\left\{I \pm m + 1\right\}\right]^{1/2} V_{\mp 1} \\
\langle m \pm 2|H_Q|m\rangle &= A\left[\left\{I \mp m\right\}\left\{I \mp m - 1\right\}\left\{I \pm m + 1\right\}\right. \\
&\qquad \left.\left\{I \pm m + 2\right\}\right]^{1/2} V_{\mp 2} \qquad (29) \\
\langle m'|H_Q|m\rangle &= 0 \quad \text{for} \quad |m' - m| > 2
\end{aligned}$$

where

$$A = \frac{eQ}{4I(2I-1)}$$

and

$$V_o = V_{zz}$$

$$V_{\pm 1} = V_{xz} \pm iV_{yz}$$

$$V_{\pm 2} = \left(1/2\right)(V_{xx} - V_{yy}) \pm iV_{xy}$$

and z is the magnetic field direction. We can write V_1 and V_2 defined by the set of equations (29), at a nuclear site due to n point charges e_n as

$$V_1 = 3\beta \Sigma_n e_n r_n^{-3} \cos\theta_n \sin\theta_n e^{i\phi_n} \qquad (30)$$

$$V_2 = (3/2)\beta \Sigma_n e_n r_n^{-3} \sin^2\theta_n e^{i2\phi_n} \qquad (31)$$

where θ_n and ϕ_n are the polar angles of the position vector of the charge e_n with respect to the z axis, β is the antishielding factor (Cohen & Reif, 1957) and the summation is taken over all the charges in the region of the nuclear site. The quantity of interest in equations (30) and (31) for this qualitative argument is θ_n. Referring to the $NaNO_3$ unit cell (Andrew et al. 1962) and supposing that H_o is applied along the crystal triad symmetry axis, the ions which provide the main contribution to the time-dependent electric field gradient at the Na^{23} sites have values of θ_n close to $\pi/2$. In this case therefore it is likely that V_2 will be greater than V_1. Since V_1 and V_2 are related to W_1 and W_2 respectively it is likely that W_2 will be greater than W_1 for the Na^{23} nucleus in $NaNO_3$ for this particular crystal orientation ($\theta = 0^\circ$). By the same argument it is likely that W_2 will be less than W_1 when the magnetic field is at right angles to the symmetry axis ($\theta = 90^\circ$).

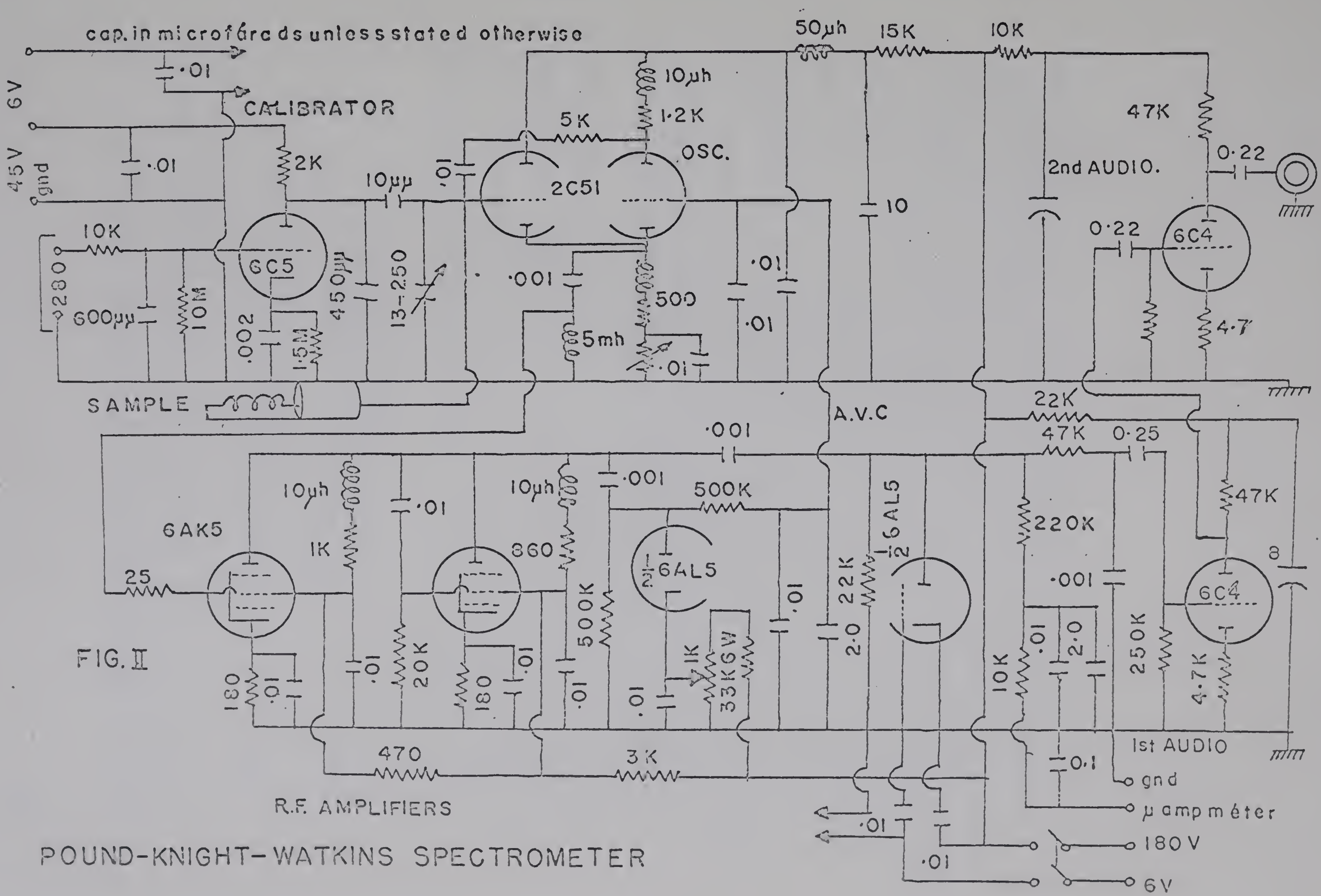

FIG. II

POUND-KNIGHT-WATKINS SPECTROMETER

III. APPARATUS

a) Spectrometer

A modified Pound-Knight-Watkins (PKW) (Watkins and Pound,1951) marginal oscillator spectrometer was built for the investigation of a single crystal of sodium nitrate. The circuit diagram of the spectrometer is given in figure II. In principle, it consists of an oscillator which executes marginal oscillations at a frequency determined by a tank circuit comprising an inductance and a capacitance in parallel. The sample is placed inside the inductance coil and the capacitance is driven by a synchronous motor via a set of precision gears to change the oscillator frequency at a suitable rate and in a uniform manner. Audio modulation of the field produces a time-dependent absorption of energy from the tank circuit as the spectrometer is swept through the resonance. The Q-factor of the tank circuit at resonance is therefore being modulated at this frequency. We have therefore an r-f amplitude modulated signal carrying information about the NMR absorption effect in the modulation side-bands. In contrast to the original PKW spectrometer, the r-f oscillation is fed from the oscillator cathode via a high-pass filter to the two r-f amplifier stages. The high-pass filter prevents

any audio signals picked up directly by the probe from reaching the r-f amplifiers. Finally, the amplitude modulated r-f signal is demodulated and amplified in a conventional manner. The audio signal from the PKW spectrometer output is then fed into a phase-sensitive detector via a narrow band amplifier which is tuned to the selected modulation frequency of 32c/sec. The 32c/sec reference voltage for the phase-sensitive detector is obtained from a phase shifting network supplying a variable voltage with a phase that can be varied between 0 and 180 degrees. The final output from this unit is then fed through a time constant circuit into a recorder.

A major problem in solid state NMR work is that of achieving an adequate signal-to-noise ratio. To help in overcoming this problem the stability of the spectrometer was ensured by using high quality stabilised power supplies for both the HT and LT. Also the HT voltage to the oscillator tube was varied to produce an optimum signal-to-noise ratio for the Na^{23} resonance in $NaNO_3$. The spectrometer was rigidly constructed from brass to minimise microphonics and provide shielding.

b) Magnet

A Varian (V-3601) magnet which employed a Hall probe as the

stabilising unit with quoted stability of 1 part in 10^6 per hour was used to provide the steady magnetic field. Field homogeneity plots were carried out for several planes in the magnet gap using a Varian probe and the Varian (VF-16B) spectrometer. This was done to obtain the position of maximum homogeneity in the magnetic field. The sample used for this work was an aqueous solution of $NaNO_3$ containing N/10 $FeCl_3$ to reduce the Na^{23} spin-lattice relaxation time thereby improving the resonance. At the same time, the stability of the magnetic field was monitored by measuring the resonance field over a period of time while the Varian r-f oscillator was locked to an external standard frequency. It was found in the early stages of this work that the stability of the magnetic field was well outside the quoted value. The fault was finally traced to the Hall probe and a replacement Hall probe enabled a field stability of a few parts in 10^6 per hour to be obtained. A further improvement was effected by totally enclosing the magnet and lagging the Hall probe leads to minimise field variations due to thermal effects. After these precautions were taken the final field stability was found to be about 2 parts in 10^6 per hour, adequate for present investigations.

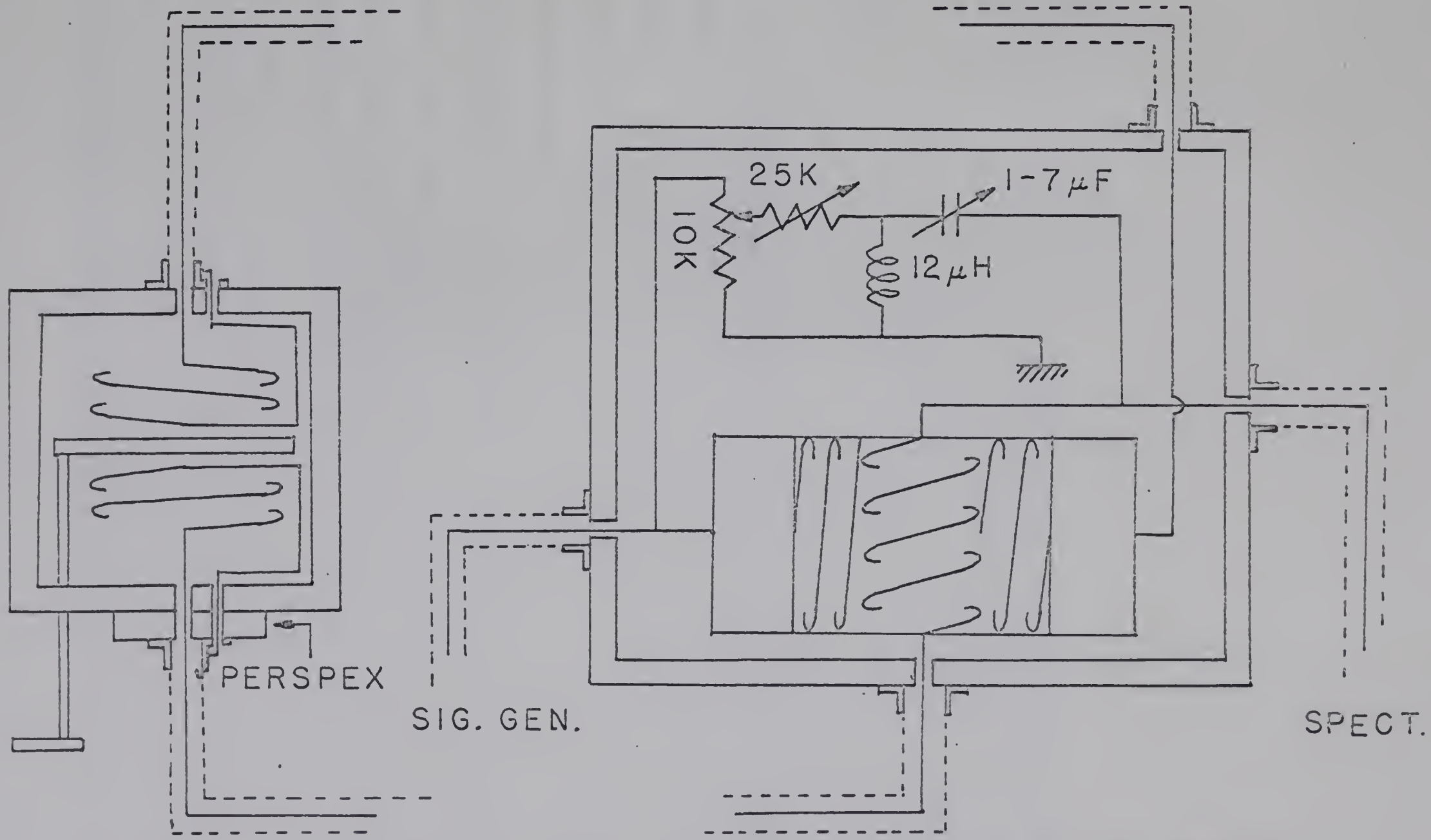

FIG III SCHEMATIC OF THE PROBE AND BALANCE MODES

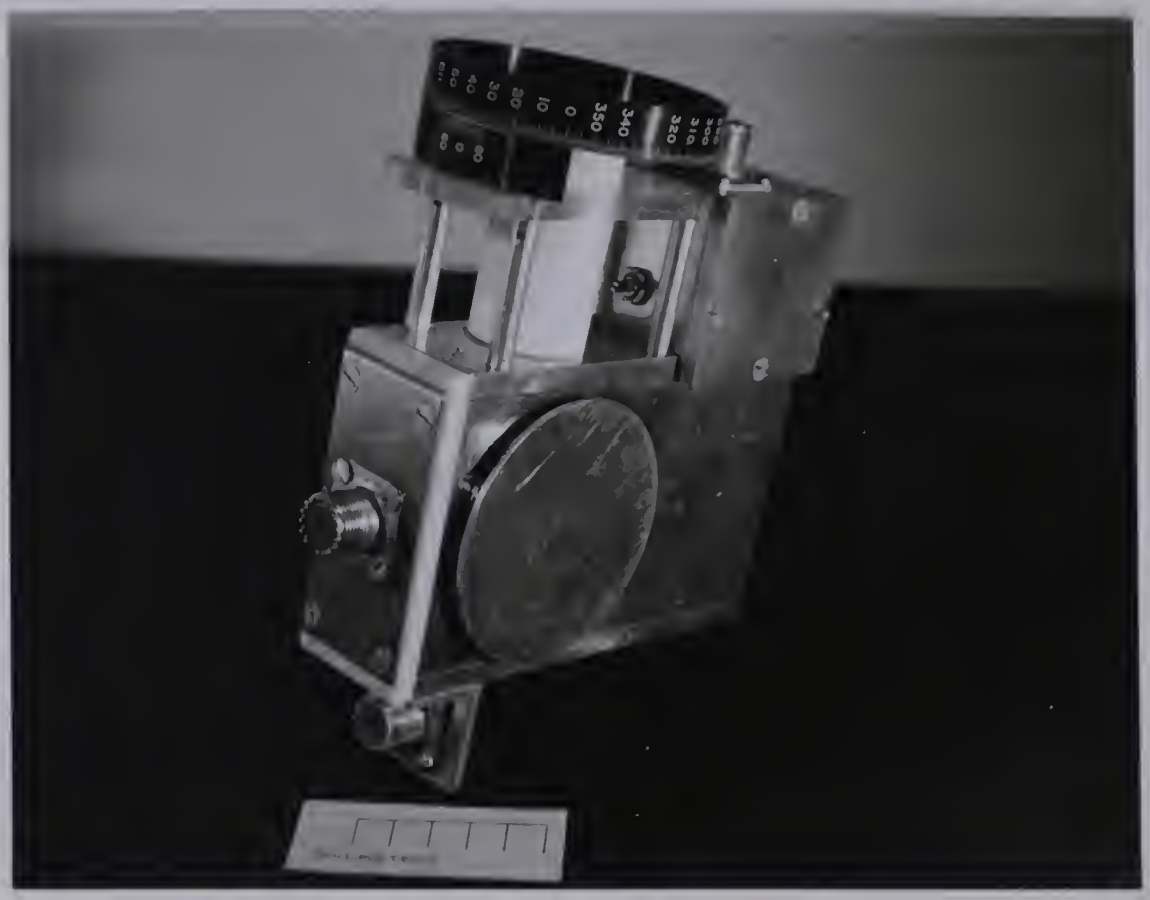
340
350
0
10
20
30
40
320
310
300

c) Probe

It was necessary to construct a probe unit to work in conjunction with the PKW spectrometer that would also offer facilities for saturating part of the spectrum at a given frequency. Since the maximum separation between a satellite and the centre line in $NaNO_3$ is 167Kc/s (Pound 1950), the prime experimental difficulty encountered was the flux leakage between the specimen coil and the transmitter coil in their approximate but not exactly orthogonal mounting. The effect of such a leakage is that when the frequency of the spectrometer gets close to the large saturating frequency it is 'driven' by the saturating voltage and no longer executes marginal oscillations at a frequency that is determined by the spectrometer tank circuit. Preliminary data taken when the leakage was still appreciable was quite erroneous.

The probe (see figure III and photograph) was milled from a solid piece of aluminium to provide the necessary rigidity and shielding. Helmholtz coils were wound to provide the modulation field on formers that had been milled on the sides of the probe body. The first method to calibrate the modulation field using a search coil proved inaccurate since the induced emf at 32c/sec was small. The second method used the fact that a severely modulated line will in the limit take the form of

a tan-curve and a width that is equal to the peak-to-peak modulation amplitude (Flynn, Seymour 1960). Therefore a modulation larger than the line width was applied to produce a tan-curve type line shape from which the modulation amplitude could be measured. It was then assumed that a linear relationship existed between the modulation field and the amplifier voltage output so that the latter could be converted to gauss.

The specimen coil was wound on a teflon former and inserted through a hole in the teflon plug around which was wound the transmitter coil, both of these coils being readily removed from the probe and altered when required. The sample was housed in a teflon holder which could be rotated about an axis perpendicular to the magnetic field. A vernier scale allowed the angular setting to be read to the nearest tenth of a degree.

d) Flux-Leakage Balance System

This system is designed to balance out the voltage induced in the specimen coil by the current in the transmitter coil. Firstly there is the voltage induced, because of the non-orthogonality of the two coils, in the specimen coil that is in phase with the transmitter

voltage. Secondly, eddy currents induced in the body of the probe, as a result of the transmitter current, induce a further voltage in the specimen coil that is in quadrature with the transmitter voltage, due to the resistive nature of the probe body. Both these voltages must be balanced out in order to avoid a 'driven' spectrometer. Following Bloch's definition (1946), the induced voltage which is in phase with the transmitter voltage is referred to as v-mode leakage and that in quadrature as u-mode.

The v-mode system is positioned outside the magnetic field and is introduced into the ground return leads of the specimen and transmitter coils (see figure III). It consists of an enclosed brass box which terminates the ground return leads in such a manner as to set up an inductive coupling which is opposite in sense to the direct mutual-inductance coupling between the specimen and transmitter coils in the probe (Blume, 1962). This coupling can be varied by means of a brass vane which rotates between the inductance loops. As the vane is rotated between the loops, eddy currents are set up in the vane and are attenuated rapidly in the material after a skin depth $\simeq$ hundred microns, thereby reducing the coupling between the two loops. Care was taken to ensure that the two inductance loops had their own ground

return paths from the brass box as illustrated in figure III.

The u-mode system is housed inside the probe. The voltage fed from this unit into the specimen coil must be in quadrature with the transmitter voltage and opposed to the quadrature voltage picked up by the specimen coil. In our case it was found necessary to employ an inductance in the unit rather than a capacitance in order to fulfill the last requirement.

The effectiveness of this leakage balance system was estimated by referring to the detector level meter which gives a measure of the r-f level in the spectrometer. The introduction of a strong saturation voltage will cause an increase in this level if the leakage is not counteracted. Hence, to avoid erroneous results due to pick-up, the balance system was adjusted so that no change in the detector level was indicated when a saturating voltage $\simeq$ 60V was applied to the transmitter coil.

e) Transmitter Voltage System

This consisted of a Marconi signal generator whose output was amplified by a tuned r-f power amplifier and then fed into the transmitter coil of the probe. The amplifier output was monitored contin-

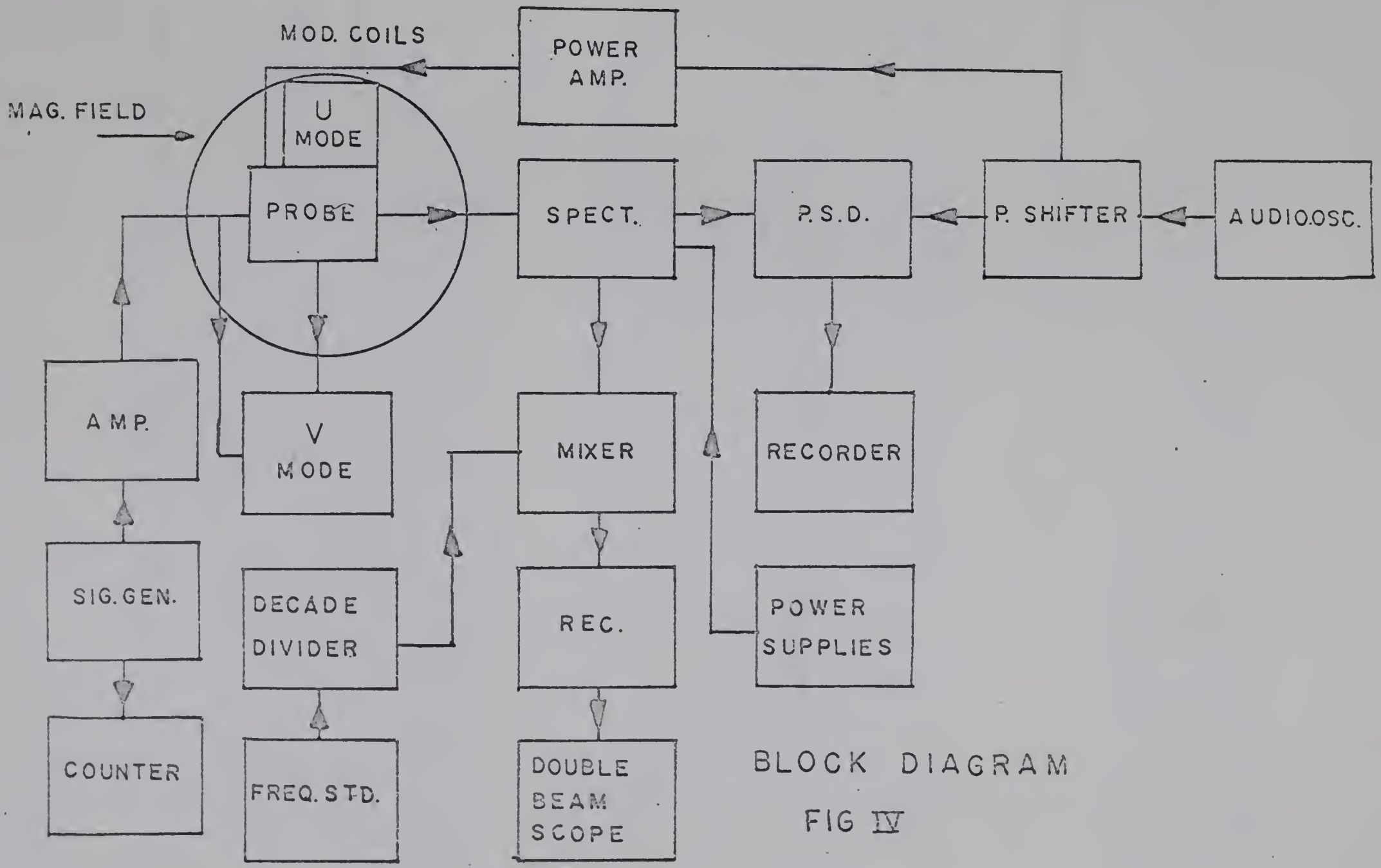

BLOCK DIAGRAM

FIG IV

uously using an oscilloscope.

f) Frequency-Marking System

This employed mixtures of fundamental and pulse outputs obtained from a decade divider system which was fed from a frequency standard. A 1 mc/sec pulse was mixed with a 10 Kc/sec pulse so as to give an extended range of 10 Kc/sec harmonics well into the r-f range. An r-f signal picked up by an aerial near the oscillator tube of the spectrometer was mixed with these harmonics and the resultant audio modulated r-f signal was fed into an Eddystone receiver. The receiver demodulated this signal to give an audio beat note the frequency of which varied as the spectrometer frequency is swept towards and away from the nearest 10 Kc/sec harmonic. The receiver was tracked to maintain maximum audio signal. The audio beat note is then fed into a double-beam oscilloscope which has 100 c/sec and 1 K/sec fundamentals from the divider as external time bases. Two sets of patterns are produced on the oscilloscope which show Lissajousfigures that allow markers to be put on the recorder chart every 100 c/sec and check markers every 1 k/sec.

A block diagram of the apparatus is shown opposite in Figure IV.

g) Sodium Nitrate Sample

The single crystal of $NaNO_3$ used in this work was in the form of a right circular cylinder, 1 cm long and 1 cm in diameter and was obtained from the Harshaw Chemical Company, Cleveland, U.S.A. The triad symmetry axis of the crystal was perpendicular to the cylinder axis and the sample was mounted in the magnet gap with the cylinder axis parallel to the axis of rotation. In this way, the angle θ could be varied from 0 to 180 degrees.

A spectroscopic analysis supplied by Harshaw showed the following impurities:

Al -3 ppm; Ca - 8 ppm; Cu < 1 ppm; Mg - 3 ppm; Si < 1 ppm.

No trace of paramagnetic ions Fe, Mn, Ni was found making the crystal suitable for the present study in that magnetic relaxation effects were negligible at room temperature.

IV. EXPERIMENTAL

The spectrum was examined and found to contain three lines of intensity roughly in a ratio 3:4:3 (as can be shown from equation 4) and have an approximate peak to peak width of 2 kc/sec indicating that this was a suitable crystal. Working at one particular crystal orientation the centre line was observed and frequency markers put on the resonance. In order to correct for the delay in response of the recorder and phase sensitive detector, the resonance was swept with frequency increasing and then for frequency decreasing. The correction was then the mean of the difference in cross-over frequency for the two cases and was found to be 100 c/sec. The angle between the triad crystal axis and the applied magnetic field was calculated from the expression $\Delta\nu_{sat} = 167(3\cos^2\theta - 1)$ (Pound, 1950) where $\Delta\nu_{sat}$ is the measured frequency separation of the satellites. For this particular orientation $\Delta\nu_{sat}$ had a value of 266 kc/sec giving a value for θ of 21.5^{o}.

Deviations from being a perfect crystal mean that a small percentage of nuclei will be in slightly different environments and will therefore have a quadrupole interaction that is different from that of the majority of the nuclei. The satellite contribution of nuclei near a crystal imperfection will be smeared out and rendered unobservable. However, the centre line is unaffected to

first order and hence there is little loss in centre line intensity due to these effects. Moreover, any loss of satellite intensity due to defects will not affect the enhancement. For these reasons we chose to saturate the centre line. The frequency of the saturating signal, which was being monitored by a frequency counter, was not allowed to drift in frequency by more than 50c/sec.

Readings of the detector level meter were converted to millivolts and the calibration curve followed the expected diode characteristic form.

For a fixed detector level the centre line was saturated with different transmitter voltages and the high frequency satellite observed. Between each run the high frequency satellite was observed when the centre line was unsaturated.

TABLE I

Unsaturated satellite peak-to-peak intensity = 4.65 ± .1 cm (the average of four runs)

Saturating Voltage Peak-To-Peak	Satellite Peak-To-Peak (cm)	Satellite Enhancement
2.0	5.55 ± .2	1.19 ± .04
3.0	6.65 ± .2	1.43 ± .04
5.0	7.15 ± .2	1.54 ± .04
6.0	7.50 ± .2	1.61 ± .04
8.0	8.05 ± .2	1.73 ± .05
10.0	8.40 ± .2	1.81 ± .05
14.0	8.05 ± .2	1.73 ± .05
20.0	8.15 ± .2	1.75 ± .05
30.0	8.05 ± .2	1.73 ± .05
40.0	8.45 ± .2	1.82 ± .05
50.0	8.25 ± .2	1.77 ± .05
60.0	8.55 ± .2	1.84 ± .05

TABLE II

For a saturating voltage of 20 volts peak-to-peak.

Detector Level (microamps)	Detector Level (millivolts)	Satellite Enhancement
3	115	1.69 ± .06
5	175	1.75 ± .07
8	270	1.76 ± .08
12	405	1.965 ± .08

FIG. V

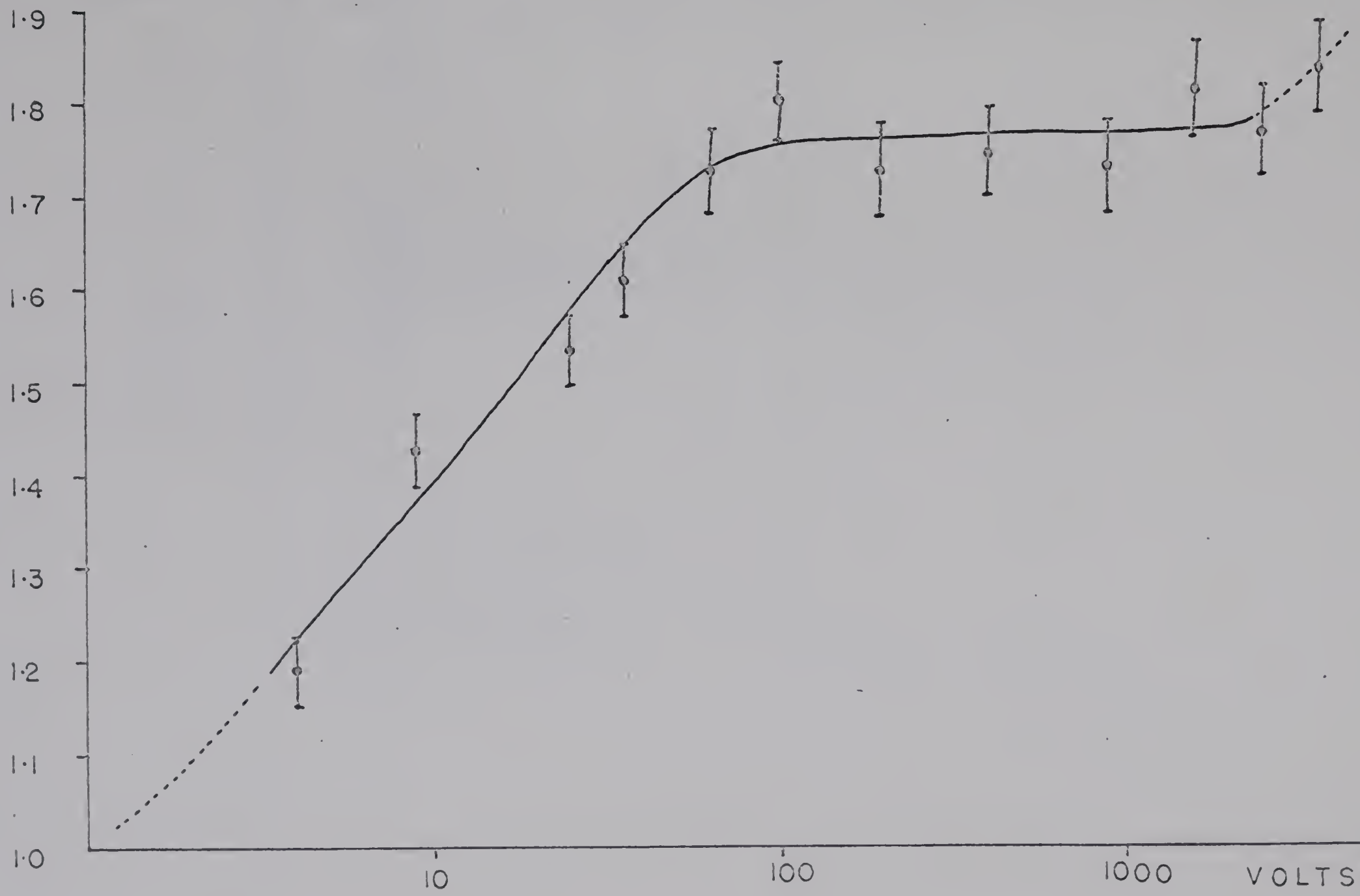
SATELLITE ENHANCEMENT
1·9
1·8
1·7
1·6
1·5
1·4
1·3
1·2
1·1
1·0
10
100
1000
VOLTS²

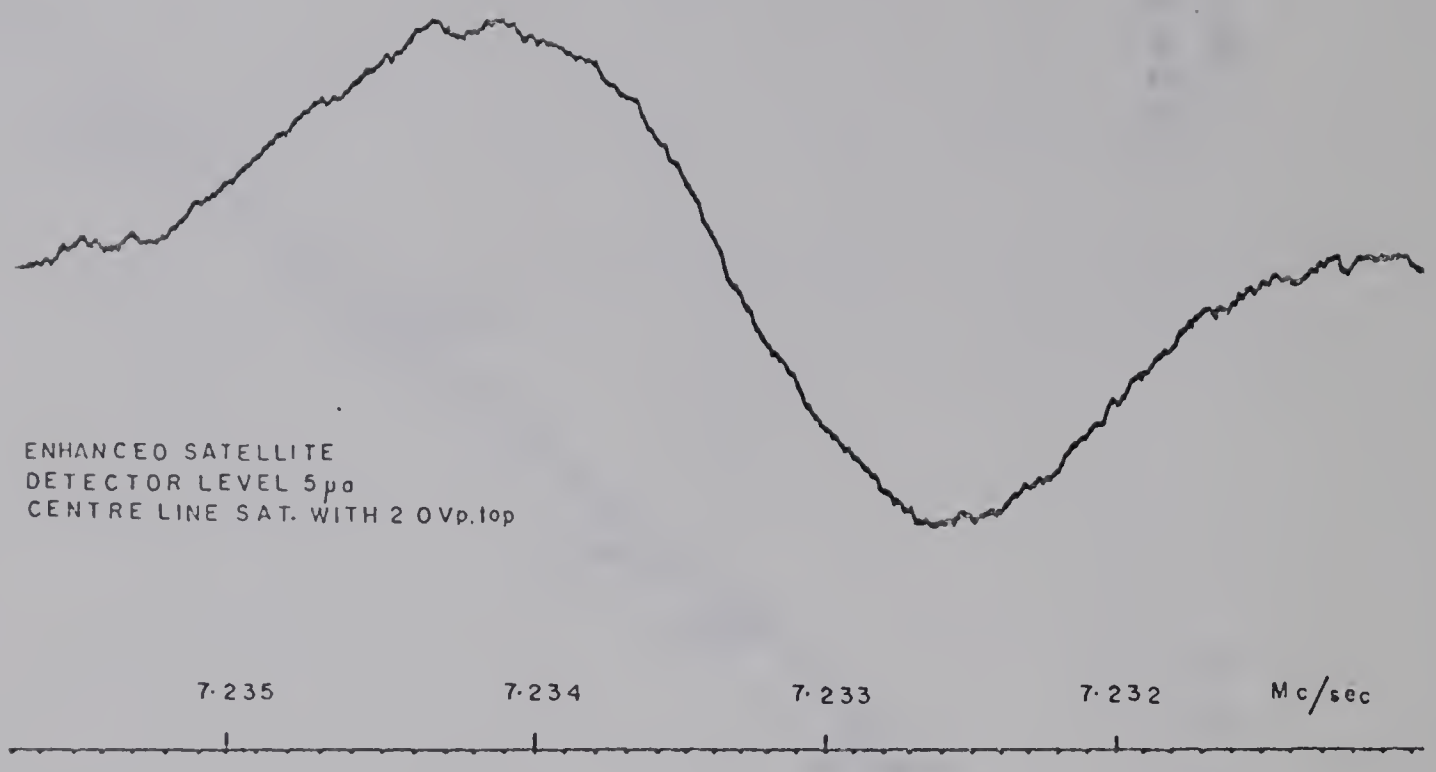
ENHANCED SATELLITE
DETECTOR LEVEL 5μa
CENTRE LINE SAT. WITH 2 0Vp.top
7·235
7·234
7·233
7·232
Mc/sec

FIG. VI

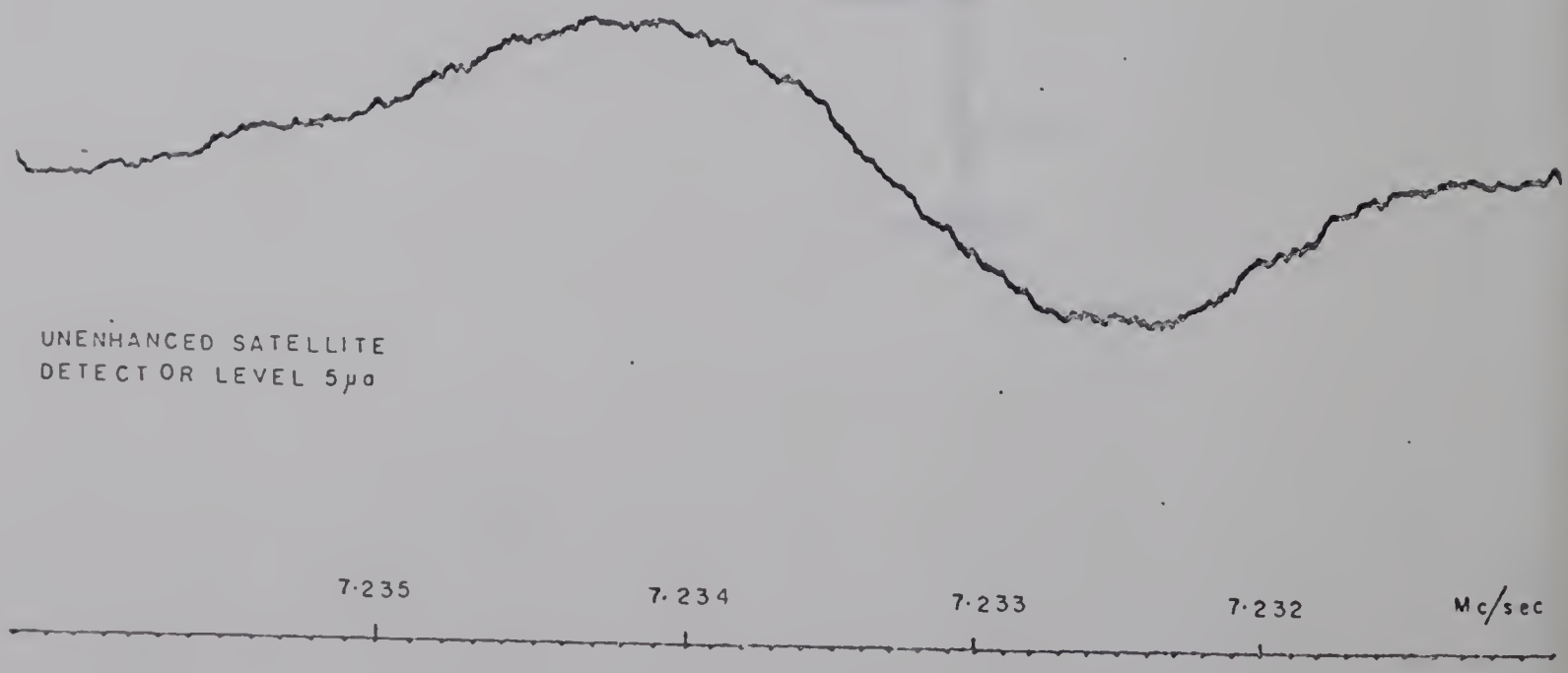
UNENHANCED SATELLITE
DETECTOR LEVEL 5μa
7·235
7·234
7·233
7·232
Mc/sec

FIG. VII

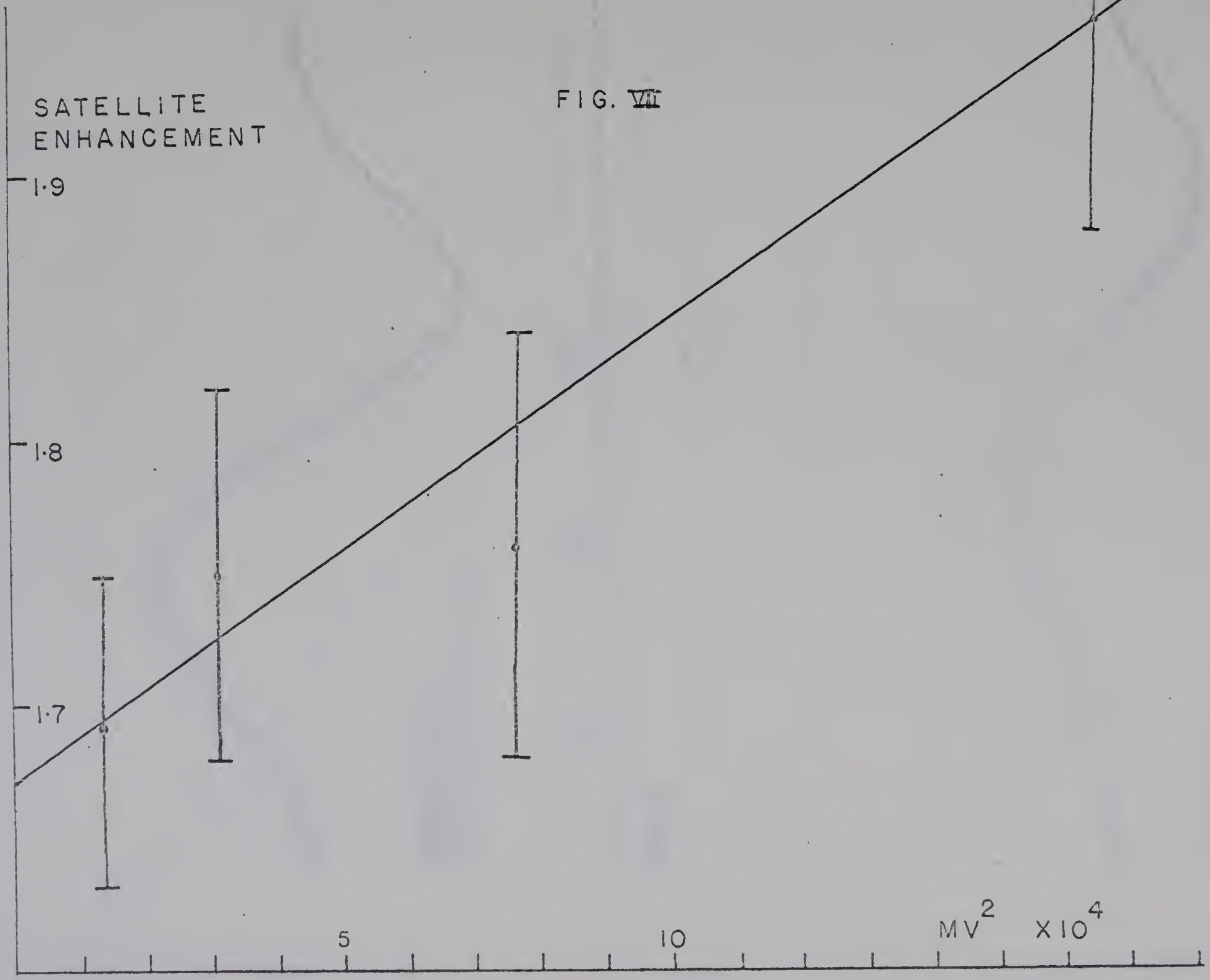

V. RESULTS

The data obtained when observing the high frequency satellite for saturated and unsaturated centre line is given in table I. The observing power during these runs was maintained at 5μa on the detector level meter. The saturating power P_{sat} is proportional to H_1^2 and H_1 is proportional to the saturation voltage. In figure V we plot the enhancement of the high frequency satellite against the square of the saturation voltage on a semi-logarithmic scale. The equations developed by Hughes (1966) predict for $P_{sat} \gg 1$ that there should be a plateau of constant enhancement. From the graph we see that this is in fact the case. We ascribe the rapid increase in enhancement for large saturating voltage as due to narrowing of the satellite line (Bloch 1958, Sarles and Cotts, 1958). Examples of a saturated and unsaturated satellite are shown in Figure VI

For a fixed saturating voltage applied to the centre line we looked at the enhancement of the high frequency satellite whilst varying the observing power. A saturating voltage of 20V peak-to-peak was chosen since this is situated near the centre of the plateau region in figure VII The data obtained is given in table II. The

observing power is plotted as the square of the detector level reading in millivolts since the observing power is proportional to H_1^2 and H_1 is proportional to the detector level in millivolts. Therefore in figure VII we have plotted the enhancement of the high frequency satellite against the representation of the observing power. The error given to each point on the graph is obtained by considering the error in estimating the peaks of the resonance on the recorder chart. This error is slightly different for each point depending on the form the resonance takes on the chart. For each detector level the enhanced resonance was measured twice and the unenhanced resonance was measured three times. The error in the enhanced case is the estimated error from the chart divided by $\sqrt{2}$ and in the case of the unenhanced it is the estimated error divided by $\sqrt{3}$. If the enhanced peak-to-peak has a value m_1 and probable error α_1 and the unenhanced peak-to-peak has a value m_2 with an associated error α_2 then the enhancement for this particular detector level is given by

$$\frac{m_1}{m_2} \pm \sqrt{\frac{\alpha_1^2}{m_2^2} + \frac{\alpha_2^2 m_1^2}{m_2^4}} \qquad (32)$$

In view of these errors and with reference to the theoretical calculation of Hughes (1966) a least square fit of the points to the function of a straight line was carried out. This straight line is shown in

figure VII.

For zero observing power the equations developed by Hughes (1966) show that the enhancement is given by

$$\frac{1 + 2x}{1 + x} \qquad (33)$$

This enhancement corresponds to the intercept on the graph in figure VII. Substitution of this value gives the ratio W_2/W_1. The value obtained for W_2/W_1 for this particular orientation and temperature is $2.1 \pm .4$. The only reported measurements on quadrupole-split Zeeman resonances are those of Goldburg (1959) who found $W_2/W_1 = 0.90 \pm .05$ at $77^{\circ}K$ for Na^{23} nuclei in sodium nitrate when the magnetic field was directed along the triad symmetry axis of the crystal. Our measurements were carried out at room temperature and on angle of 21.5° between the triad axis and applied field.

The expression for the population of a satellite when it is being subjected to an observing power p is given by Hughes (1966) as

$$N_1 = n_0\left[1 + \frac{3p(2+x)}{2(1+x)}\right]^{-1} \qquad (34)$$

where n_0 is the equilibrium population. Therefore by substituting the value of x obtained in figure VII this becomes

$$N_1 = n_0 \left[1 + 1.99p\right]^{-1}. \qquad (35)$$

From a graph of peak-to-peak intensity of a satellite against the square of the detector level, values can be taken so as to solve for B in the expression

$$N_1 = n_0 \left[1 + BV^2\right]^{-1} \qquad (36)$$

which again gives an expression for N_1. The result is an equation of the form

$$N_1 = n_0 \left[1 + 4.1 \times 10^{-5} V^2\right]. \qquad (37)$$

Equating equations (36) and (37) gives a relationship between the observing power p and the square of the detector level expressed as

$$p = 2.06 \times 10^{-5} V^2. \qquad (38)$$

The slope of the graph in figure VIIcan now be calculated in terms of enhancement against P instead of against V^2 and the result is a slope ofvalue 8.4×10^{-2}. The theoretical value is given by Hughes (1965) as

$$\frac{1+2x}{1+x}\left[1 + \frac{3px}{2(1+x)}\right] \qquad (39)$$

and substituting for x we have a slope of 1.69. The reason for such a discrepancy is not known at the present time.

VI. CONCLUSION

It has been verified that the satellite enhancement for a saturated centre line does depend on the observing power. Measurements of the enhancement for different observing powers enable the ratio W_2/W_1, for this particular orientation and temperature to be assigned the value $2.1 \pm .4$.

The reason for the discrepancy between the theoretical and experimental values for the slope of the graph of satellite enhancement against observing power is not known at the present time.

In view of the results reported by Goldburg (1959) it would appear worthwhile investigating the dependence of W_2/W_1 on the crystal orientation and temperature. The behaviour of the spectrometer and probe along with the effectiveness of the flux-leakage balance system lead us to believe that this equipment would be suitable for such an investigation.

REFERENCES

Abragam, A., 1961, The Principles of Nuclear Magnetism (Oxford: Clarendon Press), p. 411.

Andrew, E.R., 1955, Nuclear Magnetic Resonance (Cambridge University Press), p. 13.

Andrew, E.R., Eades, R.G., Hennel, J.W., Hughes, D.G., 1962, Proc. Phys. Soc., 79, 954.

Bersohn, R., 1952, J. Chem. Phys., 20, 1505.

Bloch, F., 1946, Phys. Rev., 70, 460.

Bloch, F., 1958, Phys. Rev., 111, 841.

Bloembergen, N., Purcell, E.M., Pound, R.V., 1948, Phys. Rev., 73, 679.

Blume, R.J., 1962, Rev. Sci. Inst., 33, 1472.

Cohen, M.H., Reif, F., 1957, Solid State Physics Vol. 5.

Flynn, C.P., Seymour, E.F.W., 1960, Proc. Phys. Soc., 75, 337.

Goldburg, W.I., 1959, Bull. Amer. Phys. Soc., (II), 4, 251.

Hughes, D.G., 1966, Proc. Phys. Soc., 87, 953.

Kambe. K., Ollom.J.F., 1956, J. Phys. Soc. Japan, 11, 50.

Pound, R.V., 1950, Phys. Rev., 79, 685.

Sarles, L.R., Cotts, R.M., 1958, Phys. Rev., 111, 853.

Van Vleck, J.H., 1948, Phys. Rev., 74, 1168.

Watkins, G.D., Pound, R.V., 1951, Phys. Rev., 82, 343.

Yosida, K., Moriya, T., 1956, J. Phys. Soc. Japan, 11, 33.